Title

THE PROPERTIES OF THE SPECULAR LOW ENERGY ELECTRON BEAM SCATTERED BY FACE-CENTERED CUBIC METAL SINGLE CRYSTAL SURFACES

Authors

Goodman, R.M.
Farrell, H. H.
Somorjai, G.A.

Publication Date

1967-12-01

University of California

Ernest O. Lawrence Radiation Laboratory

THE PROPERTIES OF THE SPECULAR LOW ENERGY ELECTRON BEAM SCATTERED BY FACE-CENTERED CUBIC METAL SINGLE CRYSTAL SURFACES

R. M. Goodman, H. H. Farrell and G. A. Somorjai

December 1967

DISCLAIMER

Submitted to
Journal of Chemical Physics

UCRL-17983
Preprint

UNIVERSITY OF CALIFORNIA

Lawrence Radiation Laboratory
Berkeley, California

AEC Contract No. W-7405-eng-48

THE PROPERTIES OF THE SPECULAR LOW ENERGY ELECTRON BEAM SCATTERED BY FACE-CENTERED CUBIC METAL SINGLE CRYSTAL SURFACES

R. M. Goodman, H. H. Farrell and G. A. Somorjai

December 1967

THE PROPERTIES OF THE SPECULAR LOW ENERGY ELECTRON BEAM SCATTERED BY FACE-CENTERED CUBIC METAL SINGLE CRYSTAL SURFACES

R. M. Goodman, H. H. Farrell and G. A. Somorjai

Inorganic Materials Research Division, Lawrence Radiation Laboratory
and Department of Chemistry,
University of California, Berkeley, California

ABSTRACT

The intensity, $I_{00\ell}$, of the specularly reflected low energy (10-500 eV) electron beam was monitored for the different low index crystal faces of palladium, platinum and lead as a function of electron energy (eV). The properties of the $I_{00\ell}$ (eV) curves were investigated as a function of temperature, crystal orientation, scattering angle and the appearance of different ordered surface structures. For clean surfaces, the positions of the intensity peaks were insensitive to variation of temperature. They were found to change markedly, however, with variation of the scattering angle and the formation of new surface structures on the Pd (100) face. A "reduced" electron energy scale was used to compare the intensity curves obtained for the different face-centered cubic metal surfaces. The same crystal face of the different metals yields similar intensity curves. Correlations between intensity curves from different surfaces of the same metal have also been pointed out. The occurrences of maxima and minima in the intensity of the specularly scattered low energy electron beam are primarily determined by the periodicity of the crystal lattice rather than the nature of the crystal potential. However, the relative intensities of the diffraction features are sensitive to variations in the crystal potential.

INTRODUCTION

Low energy electron diffraction (LEED) patterns resulting from the back-scattering of slow electrons (10-500 eV) from crystal surfaces reflect the periodic arrangement of atoms in the surface.[1] However, the symmetry and spacing of the diffraction features cannot unambiguously determine the position of the atoms in the crystal surface.[2] In order to uniquely determine the surface structure, one must 1) determine accurately the relative intensities of all diffraction features and 2) develop a theory which will calculate the expected relative intensities as a function of the different atomic arrangements on crystal surfaces. Only then could one differentiate between structures due to adatoms,[3] periodic lattice relaxations, ordered arrays of vacancies,[4,5] etc. and ultimately explain the mechanisms for the formation of surface structures frequently found in LEED studies.

The development of diffraction theories applicable to the scattering of low energy electrons by solid surfaces is proceeding at several laboratories.[6,7] However, such developments depend on the availability of accurate experimental intensity data. The purpose of this paper is to report some of the properties of the specular intensity (00-beam) scattered from different faces of face-centered cubic (fcc) crystals, palladium, lead, platinum, and copper.

In LEED studies, one may determine the diffraction intensity as a function of wavelength, λ, merely by changing the electron accelerating potential [$\lambda(\text{Å}) = (150.4/\text{eV})^{1/2}$]. In this paper, we present data on the wavelength dependence of the (00-beam) intensity scattered from different fcc single crystal surfaces as a function of a) temperature, b) crystal

orientation, c) the angle of incidence, and d) the presence of different surface structures. This measurement is believed to yield reliable intensity data for several reasons. 1) The (00)-reflection remains in a fixed position on the fluorescent screen as the wavelength is changed since its scattering vector is perpendicular to the surface plane. Thus, the effect of inhomogeneity of the phosphor screen, grids, window, etc. is eliminated. Furthermore, the influence of the angular dependence of the atomic scattering factor on spot intensity would not be expected to be very significant at constant scattering angles.[1,8] 2) Below about 100 eV, a large fraction of the back scattered elastic electrons reside in the specular reflection.[8] Therefore, the measurement of its intensity should be more informative than that of the other diffraction spots.

We shall indicate methods of normalizing the $I_{00\ell}(eV)$ curves to aid correlation of data taken from different materials and different orientations of the same material. Experimental difficulties are pointed out and suggestions to aid in the acquisition of future experimental data, which are important for structure analysis, will also be presented.

The $I_{00\ell}(eV)$ curves were sensitive to the angle of incidence of the electron beam, as well as to changes in surface structure. However, the intensity curves seemed quite insensitive to temperature variations. Correlations indicating similarities in the diffraction behavior of the different crystals and different crystal orientations were uncovered.

EXPERIMENTAL

The ultra-high purity fcc single crystals were used in the form of discs of approximately 0.6 cm diameter, except lead which was used in the form of a cylinder [0.7 cm long and 0.5 cm in diameter] mounted in an ultra-high purity Fe enclosure. Samples were x-ray oriented and cut to within ±1° of the desired face, etched, and polished. The LEED apparatus of the post-acceleration type[9] was used for all the measurements. With this apparatus one may monitor the intensity, $I_{00\ell}$, in an energy range of 10-500 eV and at angles of incidence (θ) from 2.5° → 23.5° to the surface normal.[29] Because of the location of the electron gun, the $I_{00\ell}$ (eV) curve cannot be measured at normal incidence. [An experimental arrangement utilizing a curved path from gun to sample and sample to screen may be used to study the specular reflection at normal incidence. As yet, no experiment of this sort has been reported, although it would be important to obtain these data.]

Since the electron beam covers approximately a 1 mm^2 area there is difficulty in obtaining reproducible data due to the variation in crystal perfection along the sample surface. One notes a large change in the overall intensity as the electron beam is scanned across the crystal. The relative intensities of the $I_{00\ell}$(eV) peaks however are fairly reproducible from different parts of the crystal. No attempts have been made to measure absolute intensities from run to run with this apparatus. Further uncertainties are introduced by beam spreading at the lowest voltages. In

taking $I_{00\ell}(eV)$ curves at elevated temperatures, effects of fields induced by heater currents cannot be ignored when resistance heating is used. This difficulty can be eliminated by using indirect heating methods, as for example, radiative heating, thermal imaging or transient techniques.[10] Considering all of these factors, most of the relative intensities of the peaks in the $I_{00\ell}(eV)$ curve were reproducible to within ±20% for given experimental conditions. Since most of the data show orders of magnitude intensity changes, the interpretations are independent of this experimental uncertainty. The measurement of the actual electron energy incident upon the crystal surface is difficult due to experimental (instrumental) uncertainties. It has frequently been observed that two identical curves obtained under the same conditions will not superimpose but are slightly shifted (2-10 volts) due to small variations in the beam voltage.

Inasmuch as the electron gun emission current may change by as much as two orders of magnitude (0.02 → 2.0 ma) over the voltage range of interest (10-500 eV), a large uncertainty in the reproducibility of the $I_{00\ell}(eV)$ curves taken with different instruments may result. For this reason, the $I_{00\ell}(eV)$ curves should be normalized for constant emission current.

Accurate intensity measurements require that the intensity detected using the fluorescent screen should be a linear function of the current density. This was found to be the case for the current densities (10^{-8}-10^{-4} amps/cm^2) and phosphor (P4 bluish-white) used in conventional LEED systems. The telephotometer used to measure the screen intensity (Gamma Scientific No. 2000 with fiber optics and variable aperture 6' → 3°) produced an output signal which was a linear function of intensity for all of the measurements. The photomultiplier output as ordinate and the

instrumental accelerating voltage as abscissa were plotted on an X-Y recorder. All measurements were carried out at 10^{-10}-10^{-9} torr ambient pressures.

RESULTS

A representative $I_{00\ell}$ (eV) curve is shown in Fig. 1a for the clean Pd (100)-(1×1) surface. The curve is plotted for an angle of incidence $\theta = 3°$ from surface normal, at a sample temperature of 300°K. Figure 1b shows the same curve replotted after normalization for constant emission current. The specular intensity is highest at lowest voltages and decreases as electron energy increases. This trend reflects the rapid decrease of the elastically scattered fraction of electrons from near unity to ~.01 over the electron energy range of interest (10-500 eV).

The curve in Fig. 1a is replotted in Fig. 1c as $I_{00\ell}$ vs. $(eV\ d^2\cos^2\theta)$, where d is the interplanar spacing[30] obtained from x-ray studies. Positions of primary Bragg peaks are indicated by arrows. It should be noted that on this "reduced" scale all materials with cubic structure will have the Bragg peaks at the same abscissa value. Such a normalizing procedure has the further convenience of making the quantity usually referred to as "inner potential" readily available.[11]

Temperature Dependence of the $I_{00\ell}$ (eV) Curves

Figure 2 shows $I_{00\ell}$ (eV) curves as a function of temperature for Pt(100) at $\theta = 2.5°$. There is no apparent change in the specular intensity curve for Pt(100) in the temperature range of this study other than a monotonic decrease in the intensity at all energies as a function of increasing temperature. This intensity decrease follows quite closely

the predictions of the Debye-Waller model.[12] One can express the temperature dependence of the intensity as $I(T) = I_0 e^{-2W}$ where I_0 is the intensity scattered by surface atoms in the absence of thermal motions and e^{-2W} is the Debye-Waller factor. The factor, (2w), can be shown[13] to be equal to $KVT \cos^2\theta/\Theta_D^2$ where $K = 12 Nh^2/Mk \cdot 150.4$ = constant for any material, M = gram atomic weight, N = Avogadro's number, k and h = Boltzmann's and Planck's constant, respectively; V = beam voltage, T = absolute temperature, θ= angle of incidence and Θ_D = effective surface Debye temperature. For platinum,[14] the decrease in Θ_D as electron energy decreases is such that the intensity of all peaks in the $I_{00\ell}(eV)$ curves decrease as approximately the same function of increasing temperature. The insensitivity of the $I_{00\ell}(eV)$ curves from clean surfaces to temperature changes correlates very well with results of surface Debye-Waller factor measurements on Pt[14] as well as on other materials (Pd,[15] Ag,[16] Pb[15]).

$I_{00\ell}(eV)$ Curves for Different Crystal Orientations

Figure 3a shows $I_{00\ell}(eV)$ curves for Pt (100), Pt (111), Pt (110) surfaces. The curves plotted on a reduced scale ($eV\, d^2 \cos^2\theta$). It is apparent that there is a strong correlation between the curves from the different surfaces, in fact, most of the peaks overlap, especially at electron energies above the position of second Bragg peak. The relative intensities of the peaks vary greatly for the different surfaces but the positions of the peaks seem to align consistently. For example, the peaks on the high energy side of the n = 3 position and the doublet straddling the arrow at n = 4 are common to all three surfaces. The (100) and (111) faces give the same peak positions near the n = 5 and the n = 6 positions.

Figure 3b shows $I_{00\ell}$(eV) curves for the three low index faces of copper[17,18] The voltage ranges for the measurements on the (110) and (100) surfaces are not large, but it is apparent that there is good correlation for the major peaks and between all of the three orientations.

$I_{00\ell}$(eV) Curves for Different Face-Centered Cubic Crystals (Pd, Pt, Pb, Cu)

Figure 4a shows $I_{00\ell}$ (eV) curves for Pt (100), Pd (100) and Cu (100) surfaces plotted on a reduced scale, (eV d^2 $\cos^2\theta$). Here the correlation between the peak positions is excellent. Most peaks in the palladium curve are present in the copper and platinum curves over a several hundred volt range - from position of about n = 2-1/2 to about n = 5. This corresponds to an electron energy range of ~60 to 250 eV for the Pd and Pt (100) surfaces. There are large differences in the relative intensities from curve to curve, but, by and large, the curves show strong similarity. Figure 4b shows the same intensity curves for the Cu (111),[17] Pt (111),[14] and Pb (111)[19] surfaces which are also plotted on a reduced scale. The Pb (111) and Pt (111) show good correlation over the short electron energy range where Pb (111) shows significant diffraction intensity.[31]

Figure 4c shows the $I_{00\ell}$ (eV) curves for Pt (110), Ni (110)[20] and Cu (110)[18] plotted on a reduced scale, (eV d^2 $\cos^2\theta$). Here the peak positions almost completely overlap and there are no peaks missing.

The relative intensities however seem to be greatly altered. At the n = 3 Bragg position, copper and platinum show a strong maximum, but nickel only a shoulder to strong maximum beyond where Pt and Cu show weaker maxima. In summary, all $I_{00\ell}$ (eV) curves [(100), (111) and (110)] show good correlation. Plotting the $I_{00\ell}$ curves on the reduced scale should yield Bragg peaks for all materials at the same positions, except for the possibilities of different "inner potential" corrections. For the materials studied there appears to be strong agreement in peak positions. Note that none of these curves have been corrected to constant emission current. We have included in the appendix a similar correlation study for PbSe and PbTe from data reported by MacRae, et al.[21]

The $I_{00\ell}$ (eV) Curves as a Function of Scattered Angle

In Fig. 5 we have plotted the $I_{00\ell}$ (eV) curves for the Pd (100)[22] face as a function of angle of incidence, θ, measured with respect to the surface normal. These curves have not been corrected for constant emission current. Interpretation of the curves is greatly simplified if one looks at their behavior within certain ranges of electron energies I(0-30 eV), II(30-60 eV), III(60-120 eV), and IV(120-190 eV). Each region is roughly centered about an expected Bragg position (10, 40, 89, 158) calculated for $\theta = 0°$. Several facts are readily apparent. Some "peaks" appear to "rotate" with θ while others do not. Splitting of peaks within regions is the primary change which occurs, with some possible correlations between certain regions. For example, peaks in regions I and III

appear to split at approximately the same angle, i.e. 25 eV and 91 eV peaks appear and disappear together. Also, some similarities exist between regions II and IV. In region II, the dominant peak at $\theta = 3°$ and 43 eV collapses with increasing θ, while peaks first at 50 eV and then at 37 eV grow in and in turn, dominate the region. In region IV, the dominant peak at $\theta = 3°$ and 141 eV gradually shifts slightly to higher electron energies and the shoulder separates into a separate peak at 131 eV; the 180 eV peak maintains its position but fluctuates in intensity; at $\theta = 13°$ the peaks at 131 and 174 eV are now bigger than the central peak at 150 eV; however, by $\theta = 16°$ the curve is very similar to the one at $\theta = 3°$ but shifted by about 15 eV. The curve at $\theta = 17\text{-}1/2°$ suggests a possible recurrence of the splittings. Regions over 190 volt seem to show definite angular effects but in no apparent correlation with the first four regions. The dominant characteristic of the curves in the high electron energy range seems to be the occurrence of severe splittings in a very narrow angular range.

In summary, the dominant effect of sample rotation on the specular intensity is the splitting and rejoining of the main peaks within regions of electron energies which center about expected Bragg peaks. Such splittings within the regions may be correlated with splittings which occur in other regions. The theories of intensity sharing[23] or shadowing[20,24] might be expected to predict this behavior as a function of rotation. Therefore, careful scrutiny of data such are presented here should help verify either or both theories. It is noted that measurements should be carried out at 1° intervals since the peaks may undergo large intensity changes within very small angular regions. Also, due to experimental

uncertainties, the measured angles are only accurate to about ±1/2°. We have not determined the azimuthal angle in the studies. Recently, Stern et al.[25] have reported on the variation of the relative peak intensities for the W (110) surface as a function of crystal rotation about the surface normal. Therefore, it is important to define the azimuthal angle, ϕ, in addition to the scattering angle, θ, in order to be able to compare the $I_{00\ell}$ (eV) vs θ data obtained for the different single crystal surfaces. We have included in the appendix a similar angular study for Pb(111).

$I_{00\ell}$ (eV) Curves in the Presence of Surface Structures

Figure 6 shows the $I_{00\ell}$ (eV) curves for the Pd (100) face in the presence of different surface structures at $\theta = 3°$ and T = 300°K. These curves have not been normalized for constant emission current. The surface structures appear as a function of heat treatment of the Pd (100) face in ultra-high vacuum.[4] After ion bombardment, the (1x1) bulk structure appears first. As the sample is progressively heated to higher temperatures and/or for longer times the pattern changes and a streaked (2x2) surface structure forms. Further heating causes the coalescence of the (2x2) streaks, to a high intensity (2x2) surface structure. At the highest temperatures (> 600°C), a further transition to a diffuse c(2x2) surface structure occurs.[32,33] It should be noted that we have investigated and determined virtually a continuum of progressive changes

in the patterns as a function of heat treatment. Simultaneously with this change in diffraction pattern, the $I_{00\ell}$ (eV) curves undergo variations (Fig. 6). In fact, the $I_{00\ell}$ (eV) curves so accurately "fingerprint" the changing surface structures that frequently changes in $I_{00\ell}$(eV) foretold transitions to different structures before they were actually visible in the diffraction pattern.

The $I_{00\ell}$ (eV) curve for the (1×1) substrate structure shows several peaks which may be indexed as Bragg peaks (n = 2 at 16, n = 3 at 77, n = 4 at 143, n = 5 at 226) if we assume shifts of about 20 eV due to electron acceleration at the crystal surface. However, many more peaks appear than these. We can see certain changes as a function of the formation of the different surface structures. Small shoulders grow in at the low energy side of the peaks, at 26, 66 and 127 eV and new peaks appear at 50 and 150 eV. Consistent with most analyses, the low electron energy region seems most sensitive to changes in surface structure. As the c(2×2) structure grows in, we see even more dramatic changes. The 143 eV and 227 eV peaks shift to higher energies and the 16 eV peaks "splits" into peaks at 16 and 20 eV. The shoulder at 127 eV in the $I_{00\ell}$ (eV) curve in the presence of the (2×2) surface structure remains weak but the 66 eV shoulder actually increases to become larger than the 77 eV peak. Similarly, the 50 eV peak seems to weaken slightly and become a shoulder of the 66 eV peak. Finally, the 26 eV peak disappears and two small peaks at 115 and 185 eV appear. To summarize these results: the presence of surface structures on the

(100) face of palladium greatly alter the $I_{00\ell}$ (eV) curves; the (2×2) structure produces shoulders on the low energy side of peaks near Bragg positions and produces completely new peaks. The c(2×2) structure shifts peaks near Bragg positions to higher electron energies, splits certain dominant peaks and leads to the formation of new peaks or greatly altered intensity ratios of existing peaks. It should be pointed out that transition structures tend to give mixtures of these characteristics, and as mentioned earlier, foretell the transformation to new structures before the new diffraction pattern actually appears.

DISCUSSION

The shape of the $I_{00\ell}$(eV) curves for the Pt (100) crystal surface remains unchanged as a function of temperature. The overall intensity of the peaks decreases with increasing temperature as predicted by the Debye-Waller formalism. These results are quite consistent with the Debye-Waller theory and previously published measurements of the surface Debye-Waller factor for several face-centered cubic metals.[14-16] The data indicate that the temperature dependence of the specular intensity is the same for all peaks including those which are at Bragg positions and those which are not.

In Figs. 3 and 4 we have plotted $I_{00\ell}$ curves obtained for different surfaces [(100), (110), and (111)] of several face-centered cubic crystals (Pt, Pb, Pd, Cu and Ni) on a "reduced" electron energy scale, (eV $d^2 \cos^2 \theta$). Plotting the curves on this scale allows one to determine the difference due to crystal potential variations without the distortions due to differences in lattice parameter or angle of beam incidence. For the materials studied, the $I_{00\ell}$(eV) curves are very similar, the peak positions frequently overlap. This indicates that the scattering of low energy electrons is more dependent on the basic symmetry of the substrate than on the peculiarities of the atomic potentials for the different face-centered cubic metals. This seems generally valid for HEED (high energy electron diffraction)[26] and x-ray scattering[27] as well. The differences in crystal potential for different fcc metals seem to modulate the intensities of the various peaks. The shadowing models,[1,20] suggest significant differences in the $I_{00\ell}$(eV) curves for the different crystal orientation;

the curves in Figs. 3a and 3b do indicate that similarities in the intensity curves for the different faces are more extensive than predicted by this model. It should be noted however, that the differences in voltage at which the "2/3" or "1/2" order peaks appear may be sufficiently small so as to be obscured in the reduced plot. If we assume intensity sharing[23] between the different diffraction beams or multiple scattering[6] many of the dominant features of the $I_{00\ell}(eV)$ curves can be explained and predicted. The interpretation of the intensity curves based on the intensity sharing model hinges on the appearance of minima when other beams undergo maxima. If peak splittings change with rotation in the predicted manner, it would be a strong support for this theory. Finally, the intensity changes which are due to the particular material may alter some of the specific details, for example, by enhancing the intensity of one peak while diminishing that of another. Such effects may be checked by comparing line shapes - the data presented do indicate such possibilities.

The $I_{00\ell}(eV)$ curves for the Pd (100) crystal surface change both as a function of surface structural changes and as a function of scattering angle. The prominent effects in both cases are the splitting of the main peaks and the production of new peaks at certain electron energies characteristic of a given surface structure or angle of incidence, respectively. The sensitivity of the $I_{00\ell}(eV)$ curves to changes of scattering angle or surface structure should lead to an improved ability to test theoretical predictions.

Although the $I_{00\ell}$ (eV) curves contain valuable information which will help to shed light on the nature of low energy electron diffraction it is important to note some of the limitations of this type of experiment.

It is very difficult to discuss the properties of one or even two diffracted electron beams as a function of wavelength without following the intensities of most of the other diffracted beams of the same time. The $I_{00\ell}$(eV) curve should be a function of all the other $I_{nk\ell}$ (eV) curves. In order to carry out structure analysis it seems that one should monitor the total diffracted intensity which is scattered into the different order diffraction spots as a function of wavelength. Such experiments are in progress. Fluctuations in the total intensity as a function of wavelength may also indicate the diffraction conditions necessary to optimize the back-reflection of elastic electrons.

In order to correlate relative intensity data from studies which are carried out in different laboratories, the $I_{00\ell}$ (eV) curves should be normalized for constant emission current. The experimental conditions should be well defined (clean surface, etc.) and variables such as the azimuthal angle should be reported. It should be noted that intensity measurements which involve sample rotation with respect to the surface normal are affected by the variation of the atomic scattering factor, $f(\theta)$.

ACKNOWLEDGMENTS

This work was supported by the United States Atomic Energy Commission.

REFERENCES

1. J. J. Lander, Progr. Solid State Chem. 26, 2 (1965).
2. E. G. Bauer in Adsorption et Croissance Cristalline, (Editions du Centre de la Recherche Scientifique, Paris, 1965).
3. J. J. Lander and J. Morrison, J. Appl. Phys. 34, 1403 (1963).
4. A. M. Mattera, R. M. Goodman, G. A. Somorjai, Surface Sci., 7, 26 (1967).
5. H. B. Lyon, Jr. and G. A. Somorjai, J. Chem. Phys. 46 (7), 2539 (1967).
6. E. G. McRae, Surface Sci. 8, 14 (1967).
7. K. Hirabayashi and Y. Takeishi, Surface Sci. 4, 150 (1966).
8. J. J. Lander and J. Morrison, J. Appl. Phys. 34 (12), 3517 (1963).
9. Instrument manufactured by Varian Associates, Palo Alto, California.
10. R. M. Goodman, to be presented at American Crystallographic Association meeting in Tucson, Arizona, February 1968.
11. B. K. Vainshtein, Structure Analysis by Electron Diffraction, (Pergamon Press, New York, 1964).
12. I. Waller, Z. fur Physik, 17, 398 (1923).
13. J. M. Ziman, Principles of the Theory of Solids, (Cambridge University Press, Cambridge, 1964).
14. H. B. Lyon, Jr. and G. A. Somorjai, J. Chem. Phys. 44 (10), 3707 (1966).
15. R. M. Goodman, H. H. Farrell, and G. A. Somorjai, to be published.
16. E. R. Jones, J. T. McKinney, and M. B. Webb, Phys. Rev. 151A (2), 476 (1966).
17. N. J. Taylor, Surface Sci. 4, 161 (1966).
18. G. W. Simmons, D. F. Mitchell, and K. R. Lawless, Surface Sci. 8, 130 (1967).

19. R. M. Goodman, unpublished data from this laboratory.

20. R. L. Gerlach and T. N. Rhodin, Surface Sci. 8, 1 (1967).

21. D. C. Johnson and A. U. MacRae, J. Appl. Phys. 37, 2298 (1966).

22. H. H. Farrell and R. M. Goodman, unpublished data from this laboratory.

23. T. M. French, H. H. Farrell and G. A. Somorjai, to be published.

24. I. H. Khan, J. P. Hobson, and R. A. Armstrong, Phys. Rev. 129A, 1513 (1963).

25. A. Gervais, R. M. Stern, M. Menes, given at 27th Annual Physical Electronics Conference, March 1967.

26. Upon standing at room temperature, the diffuse c(2×2) pattern becomes sharp and very intense. Reheating to > 500°C causes the pattern to become diffuse again. This is probably associated with greater disorder at higher temperatures. By contrast, if the c(2×2) is heated to between about 200 and 400°C, the (2×2) surface structure is regenerated. However, if both the c(2×2) and the (2×2) are present on the sample surface at room temperature, the c(2×2) will gradually spread until, after several days, it completely covers the surface. The (1×1) may easily be regenerated by very short ion bombardments, but not by thermal treatment.

27. R. D. Heidenreich, Fundamentals of Transmission Electron Microscopy, (Interscience, New York, 1964).

28. R. W. James, The Optical Principles of the Diffraction of X-Rays, (G. Bell and Sons, London, 1965).

29. Here θ refers to the angle of incidence = 1/2 angle measured on screen.

30. For example, if a = bulk lattice parameter, then $d_{(100)} = 1/2\ a$; $d_{(110)} = 1/4\ a\sqrt{2}$, $d_{(111)} = 1/3\ a\sqrt{3}$.

31. Due to the large Debye-Waller factor the scattered intensity from lead surfaces decreases rapidly with increasing electron energy and becomes undetectable over 150 eV.

32. The pattern designated Pd (100) - c(2×2) consists of normal (1×1) with extra spots at the centers of squares of the (1×1) pattern. For consistency this pattern should perhaps be labelled c(1×1) however, in the literature it has generally been designated c(2×2) and we shall follow this precedent.

33. R. L. Park and H. H. Madden, Jr., private communication.

34. E. G. McRae and C. W. Caldwell, Jr., Surface Sci. 2, 509 (1964).

APPENDIX

Figures A-laand A1b show $I_{00\ell}$ curves for the (100) faces of lead selenide and lead telluride at $\theta = 3°$ and $\theta = 6°$, respectively, as a function of reduced electron energy from the work of Johnson and MacRae.[21] Correlations of peak psotions between the different materials are good, especially at the lower beam voltages. However, as with the fcc metals, the relative peak intensities vary from material to material. In addition, comparing Fig. A-1a with A-1b shows that changes in the $I_{00\ell}$ (eV) curves with angle of incidence do occur. Thus, the $I_{00\ell}$(eV) curves of the salts studied show similar properties to those curves for the fcc metals. Similar study on LiF[34] was not included because of the short energy range of the data.

Figure A-2 shows the $I_{00\ell}$(eV) curves for the (111)-face of lead plotted as a function of angle of incidence θ. Note the change of scale above 50 eV. These curves were not corrected for constant emission. Perhaps the most striking feature of these curves is the strong effect of the Debye-Waller factor. Thermal diffuse scattering dominates above about 125 eV. As demonstrated in Fig. 5 [on Pd (100)], the effect of the angle of incidence on the $I_{00\ell}$ (eV) curves is very marked. For example on the Pb (111) there is no peak at 70 eV for $\theta = 3°$. A peak appears however with increasing intensity as θ increases. Also, the shoulder at about 30 eV increases as θ increases.

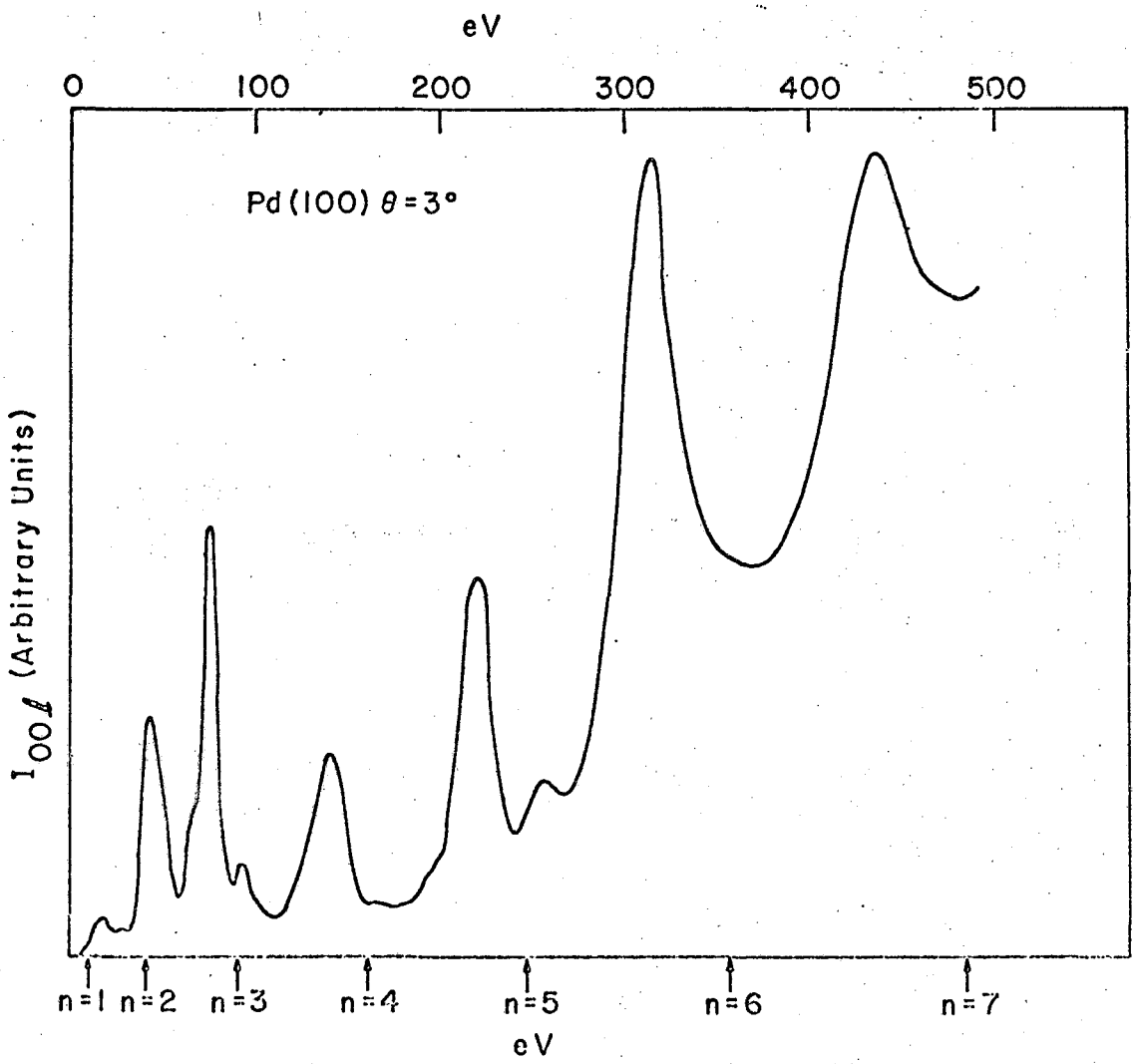

XBL 681-30

Fig. 1a Specular intensity as a function of beam voltage for (100) face of palladium. The weak shoulders at 49 and 65 eV are associated with the incipient formation of a 2×2 surface structure (see Fig. 6).

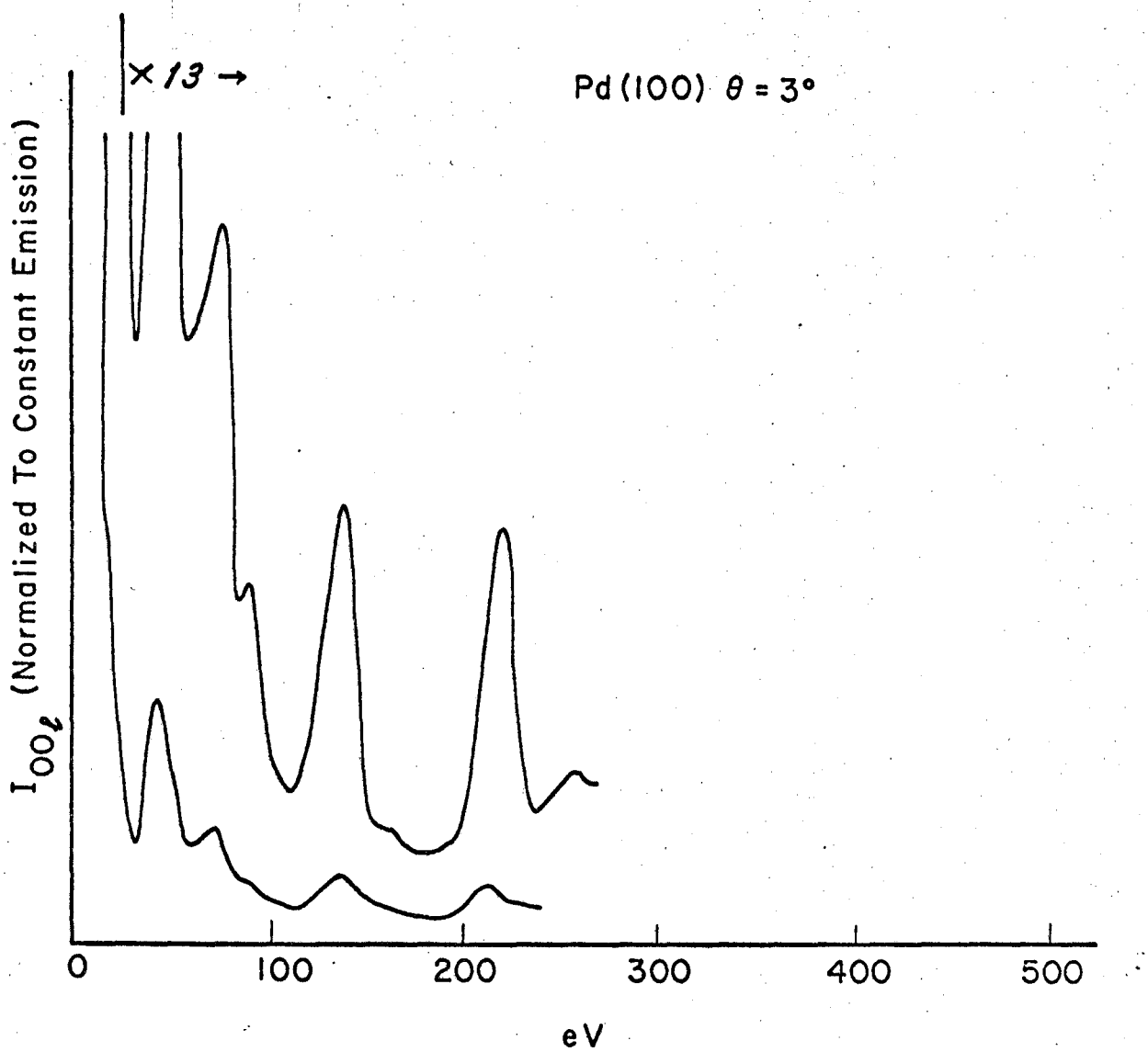

XBL 681-31

Fig. 1b Specular intensity as a function of beam voltage for (100) face of palladium at constant electron gun emission current. Note the change of scale on the intensity axis.

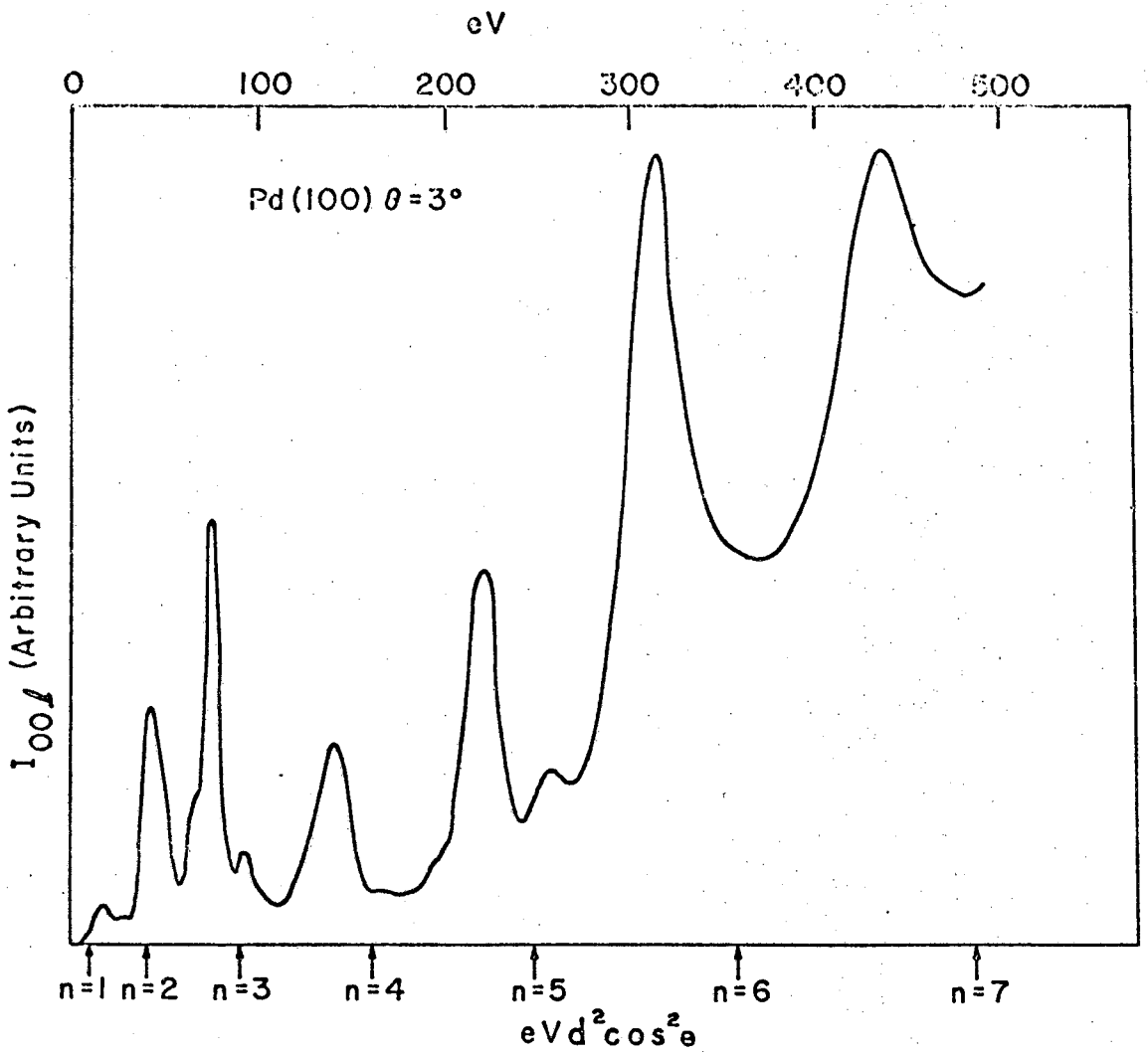

Fig. 1c Specular intensity as a function of reduced electron energy for (100) face of palladium

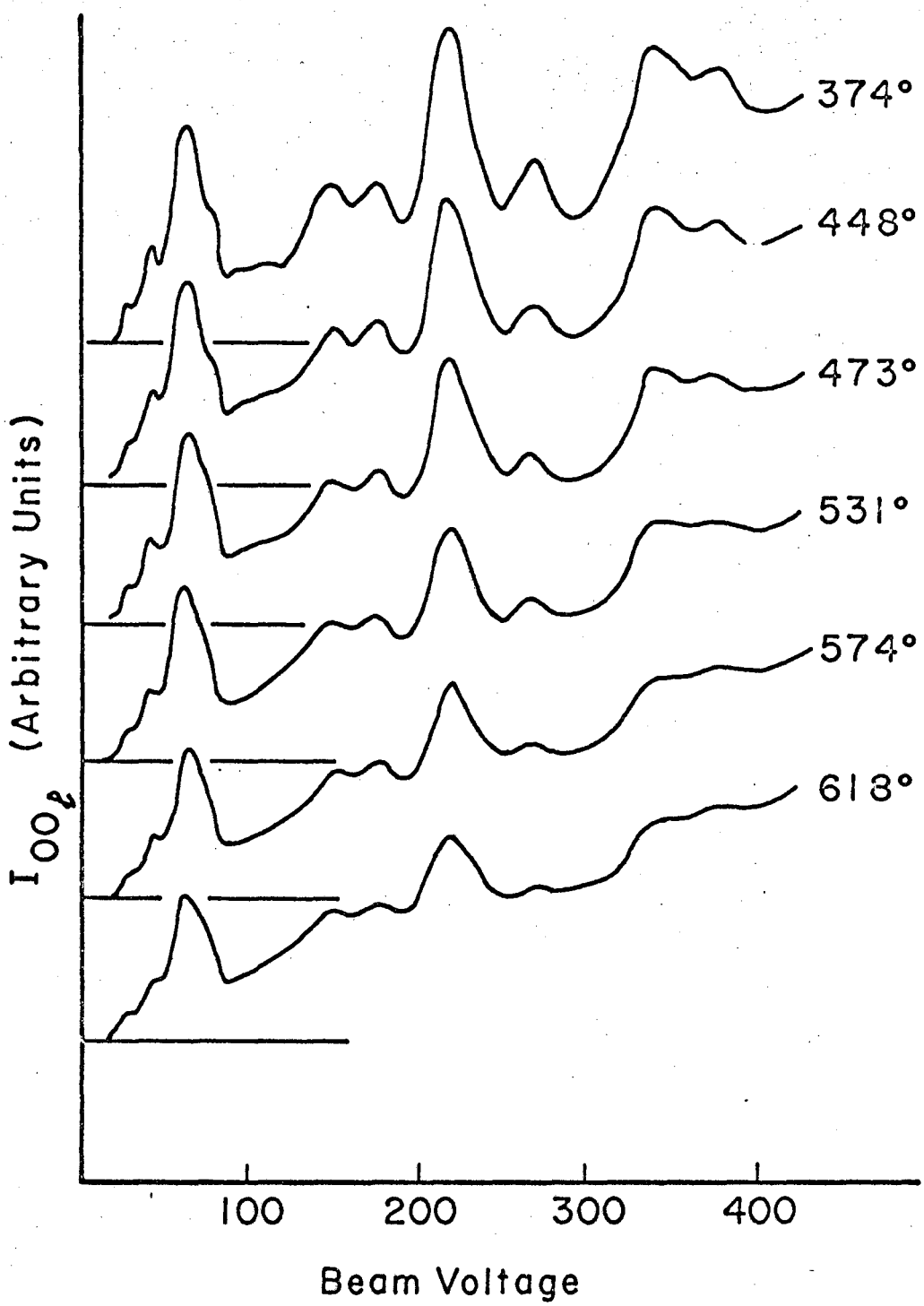

XBL 681-33

Fig. 2 Specular intensity as a function of beam voltage for (100) face of platinum at different sample temperatures

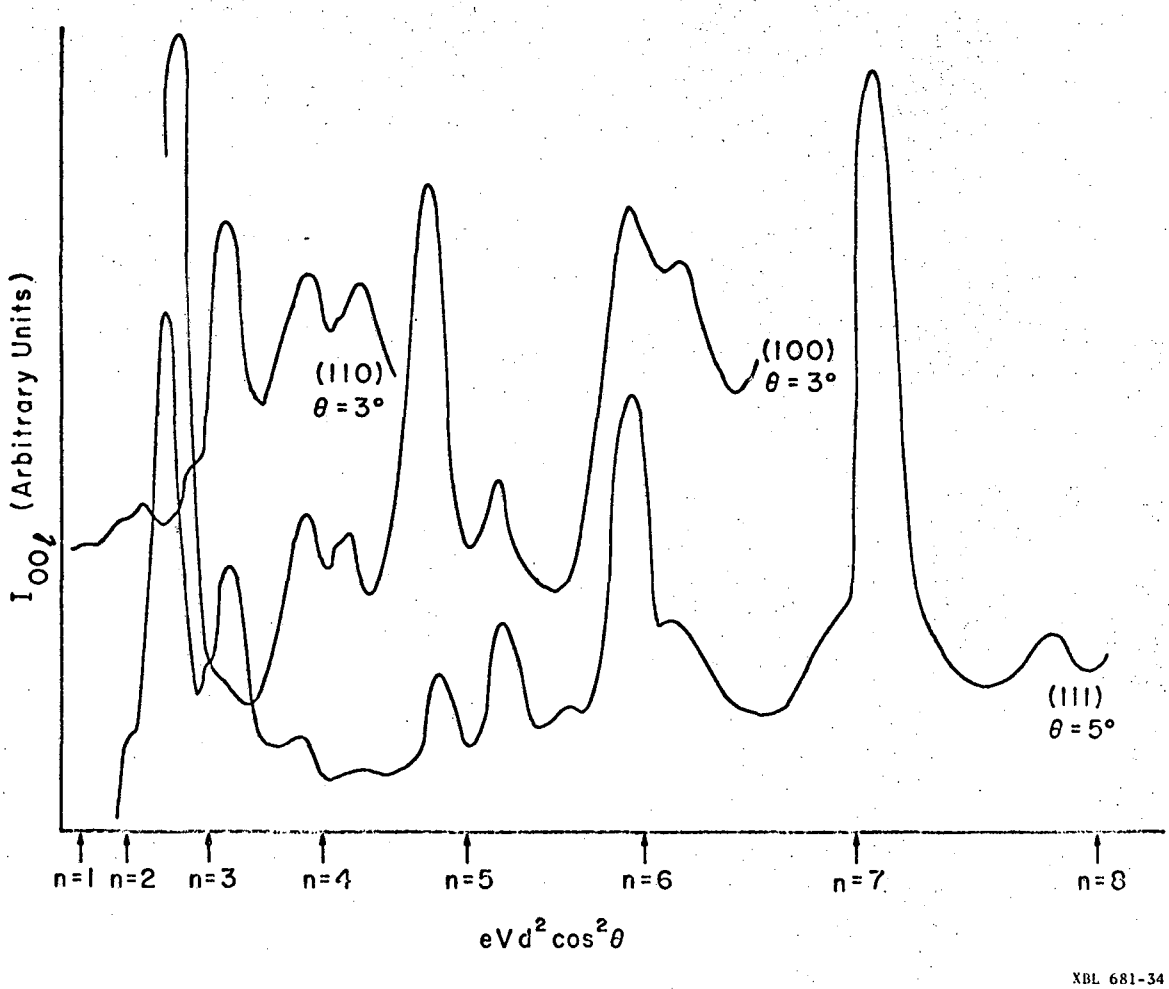

Fig. 3a Specular intensity as a function of reduced electron energy for (100), (111) and (110) faces of platinum.

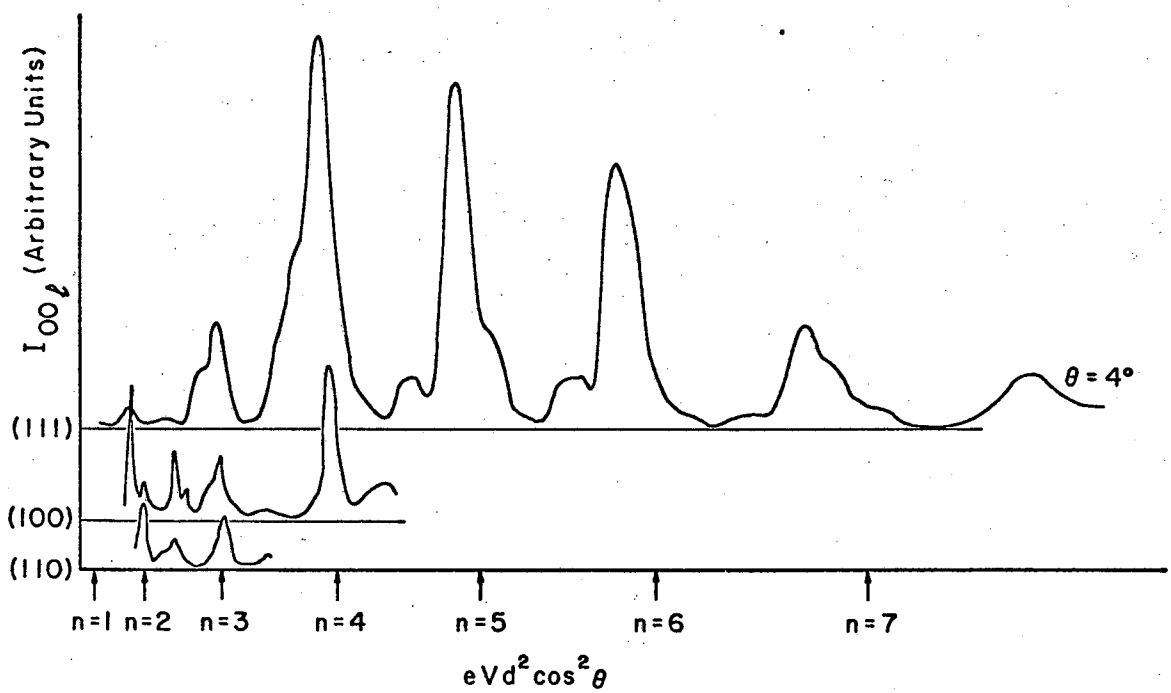

XBL 681-35

Fig. 3b Specular intensity as a function of reduced electron energy for (100), (111) and (110) faces of copper.

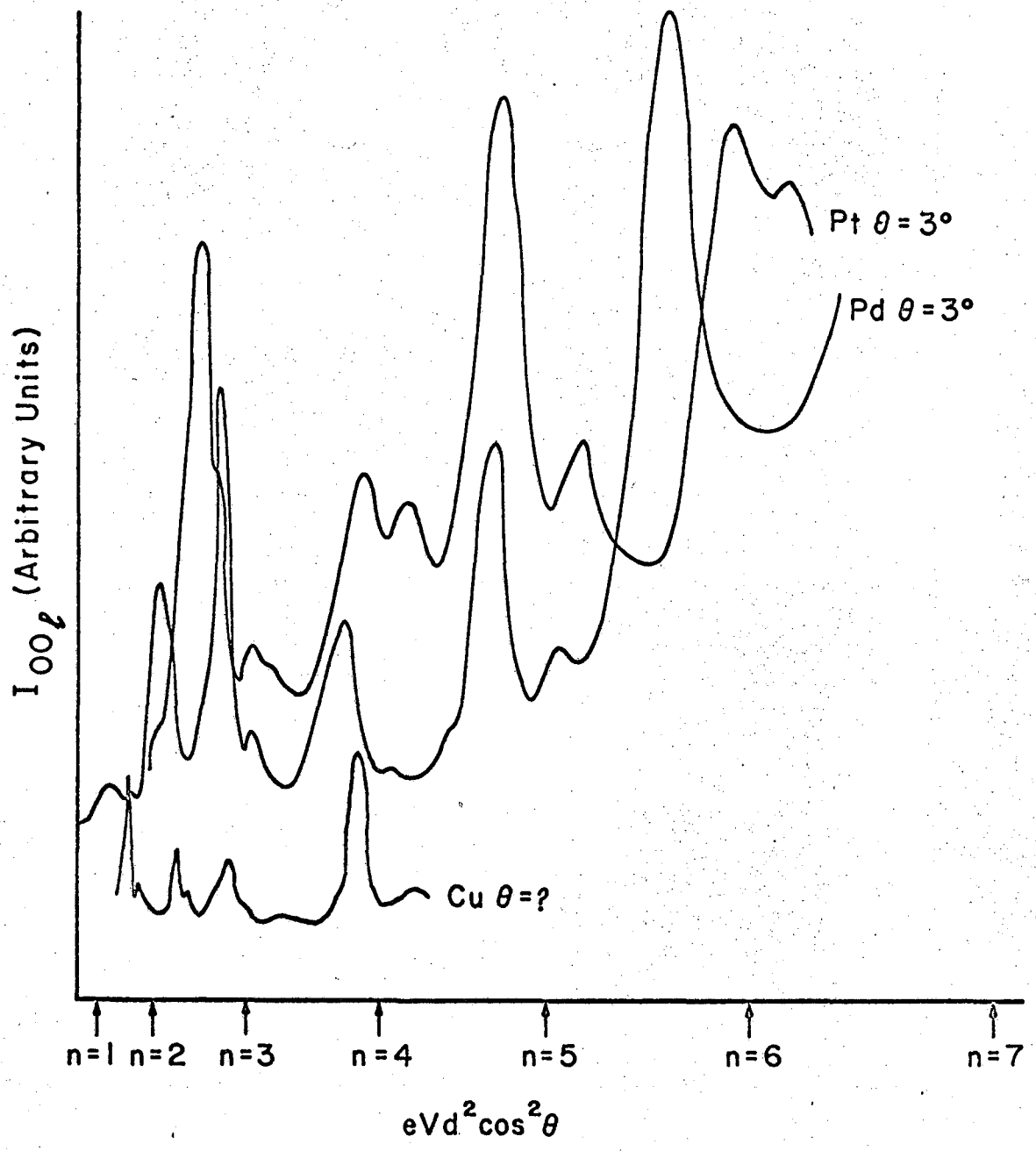

XBL 681-36

Fig. 4a Specular intensity as a function of reduced electron energy for (100) faces of platinum, palladium and copper.

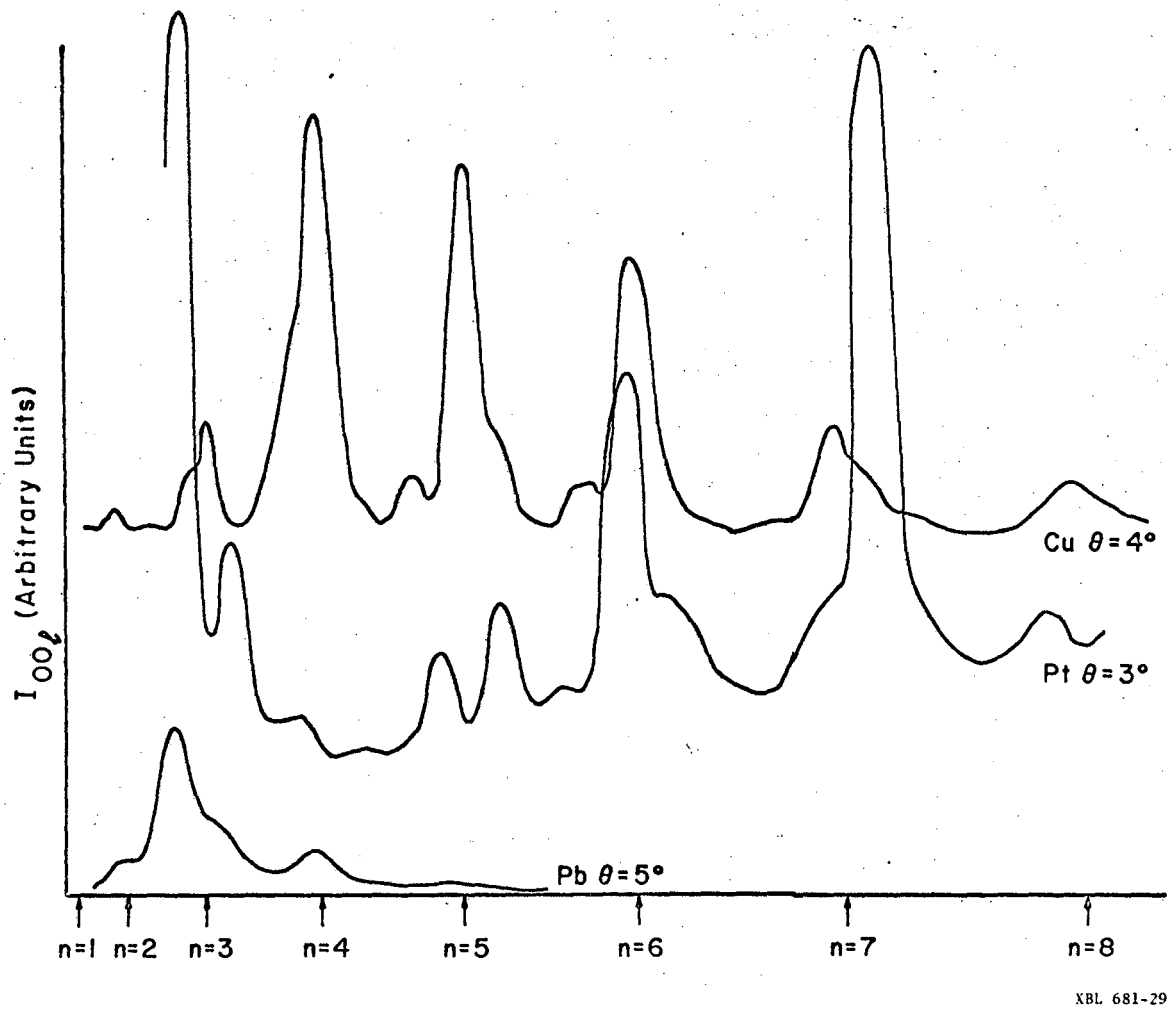

Fig. 4b Specular intensity as a function of reduced electron energy for (111) faces of platinum, copper and lead.

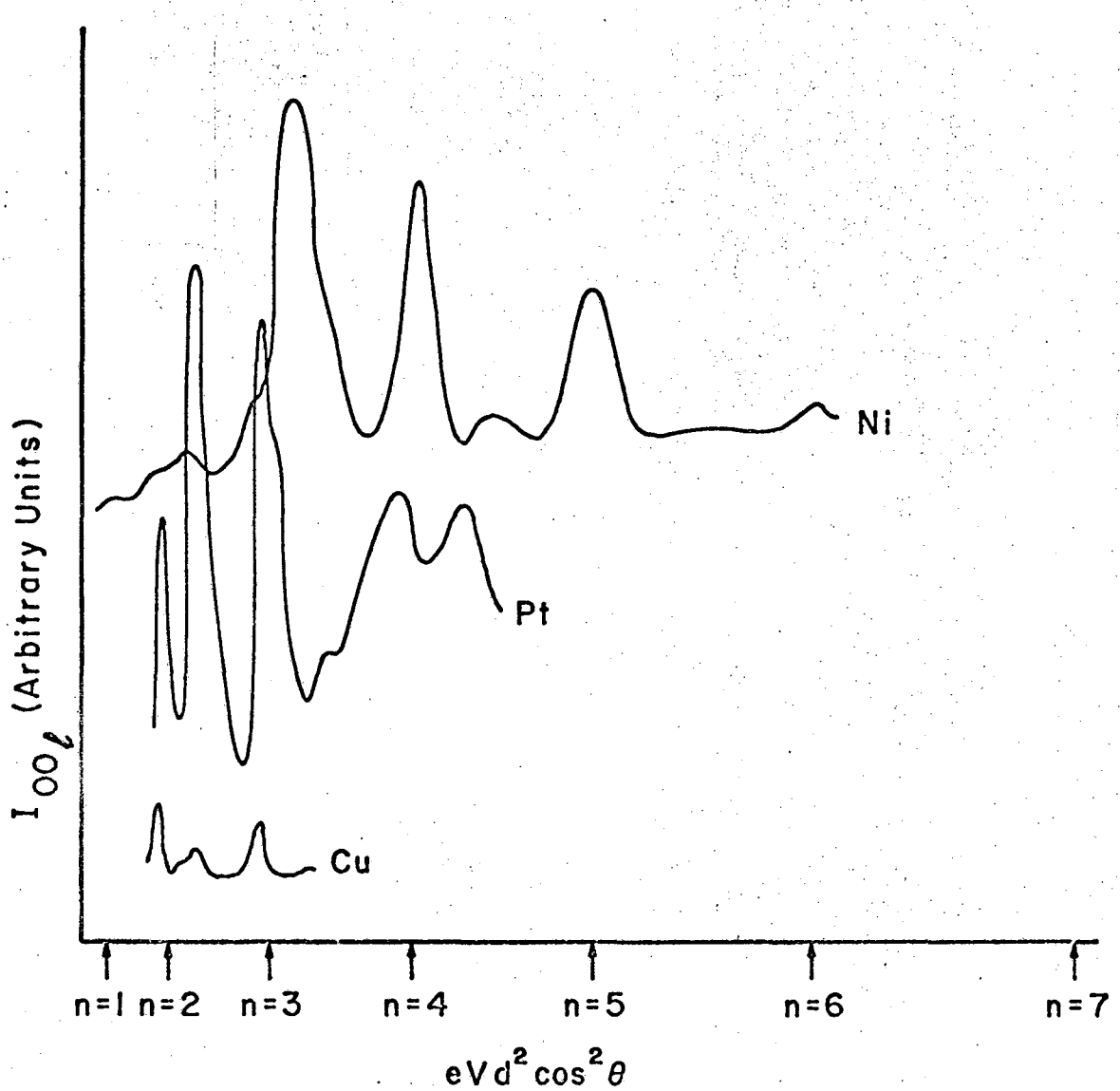

XBL 681-28

Fig. 4c Specular intensity as a function of reduced electron energy for (110) faces of platinum, copper and nickel.

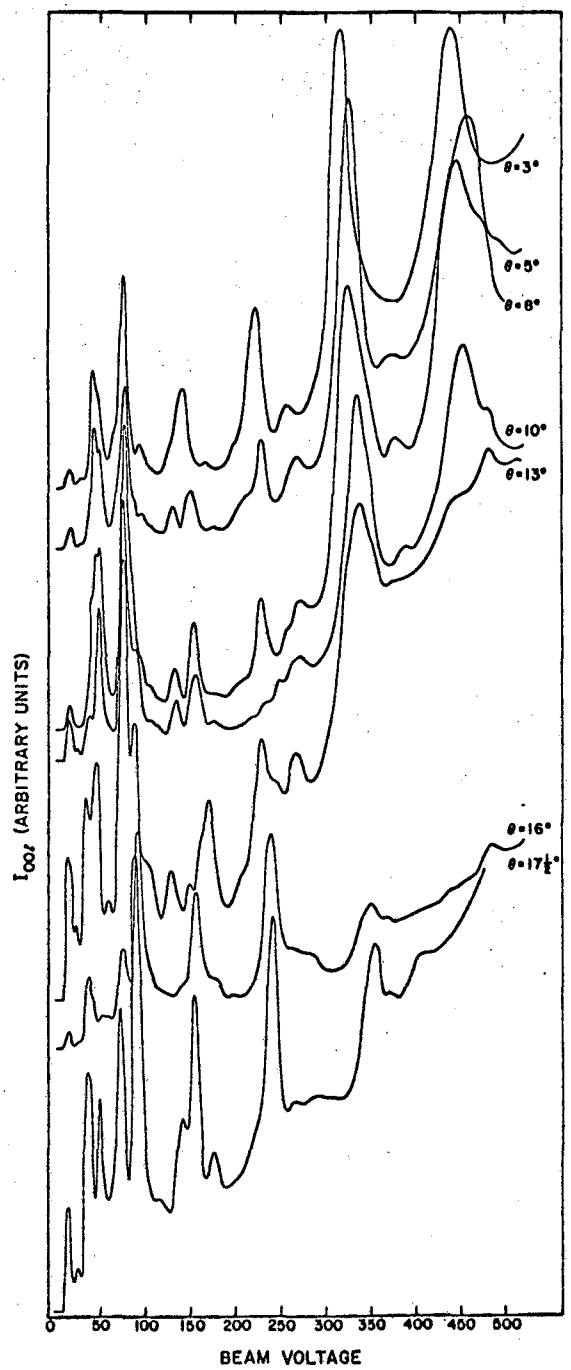

XBL 681-27

Fig. 5 Specular intensity as a function of beam voltage for the (100) face of palladium at different angles of incidence.

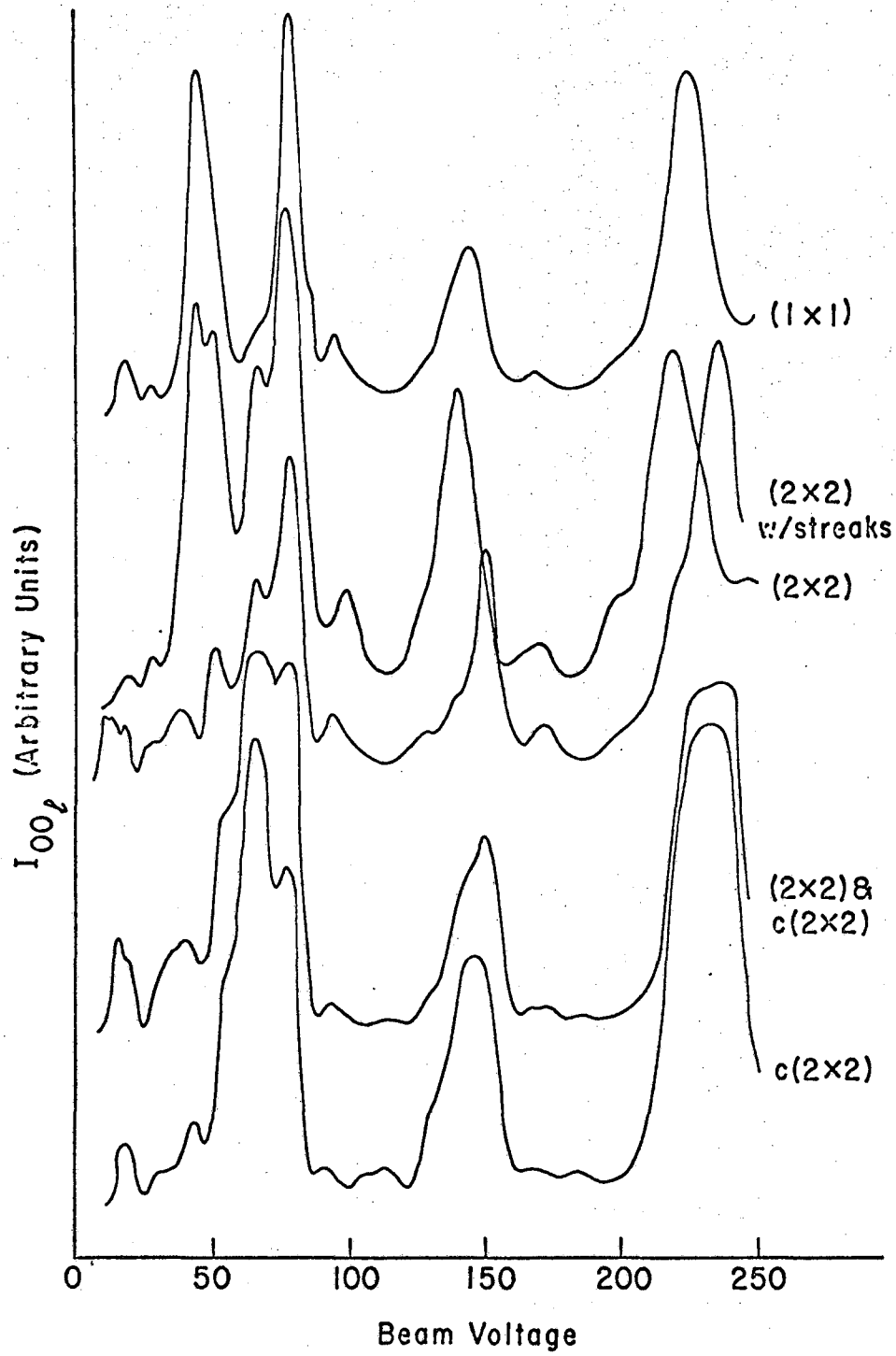

Fig. 6 Specular intensity as a function of beam voltage for the (100) face of palldium in presence of different surface structures.

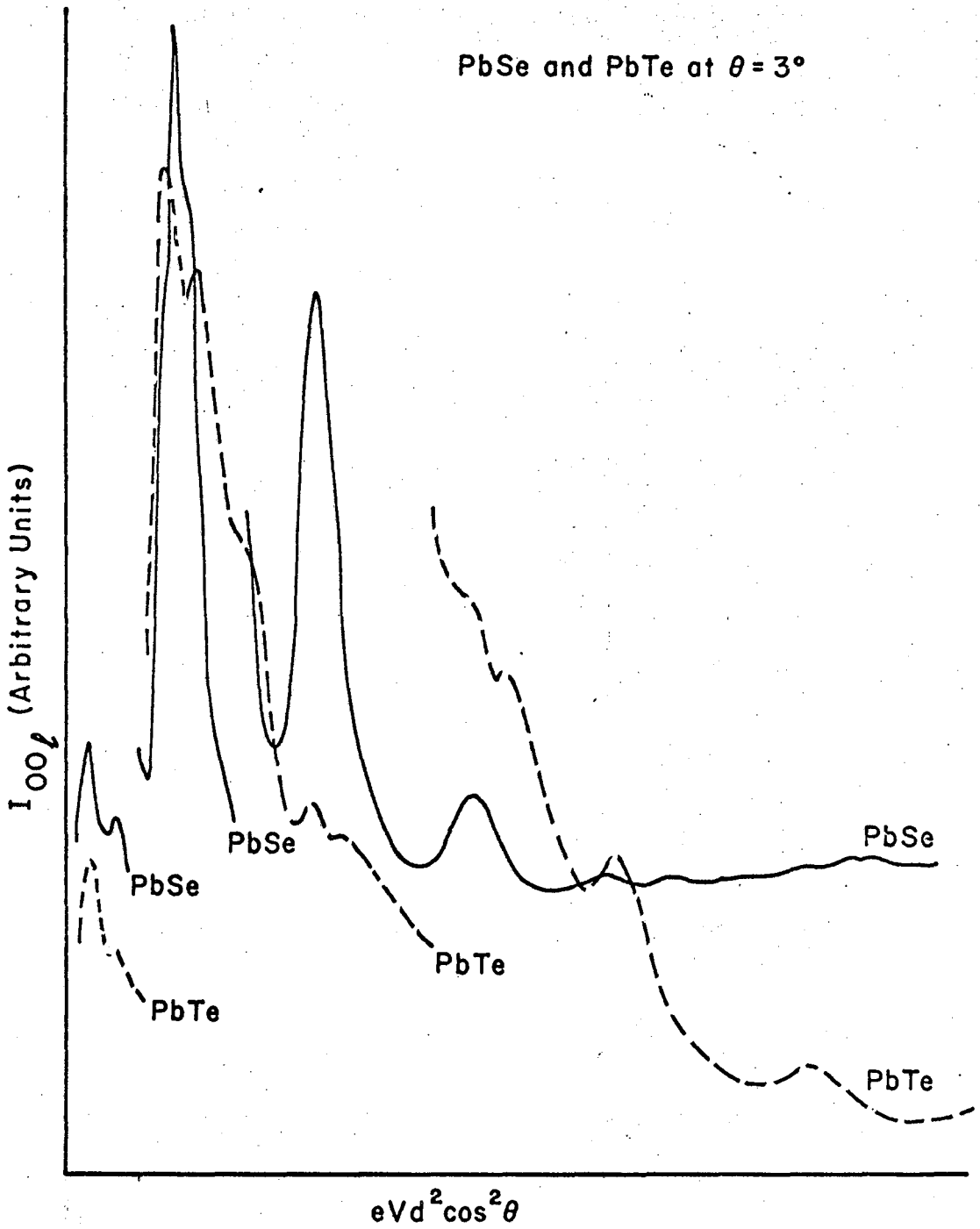

XBL 681-26

Fig. A-1 (a) Specular intensity as a function of reduced electron energy for (100) faces of lead selenide and lead telluride at an angle of incidence of 3°.

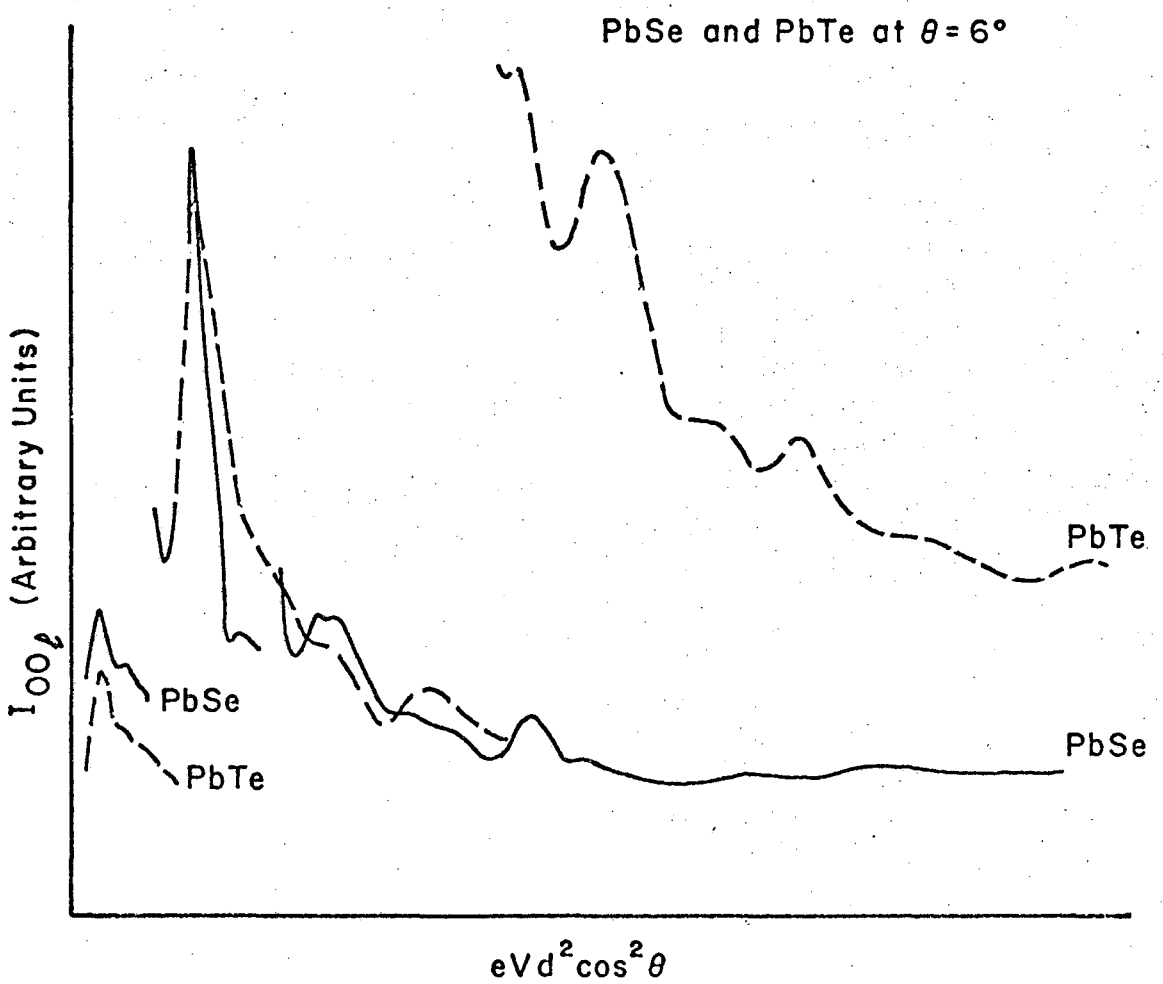

XBL 681-25

Fig. A-1 (b) Specular intensity as a function of reduced electron energy for (100) faces of lead selenide and lead telluride at an angle of incidence of 6°.

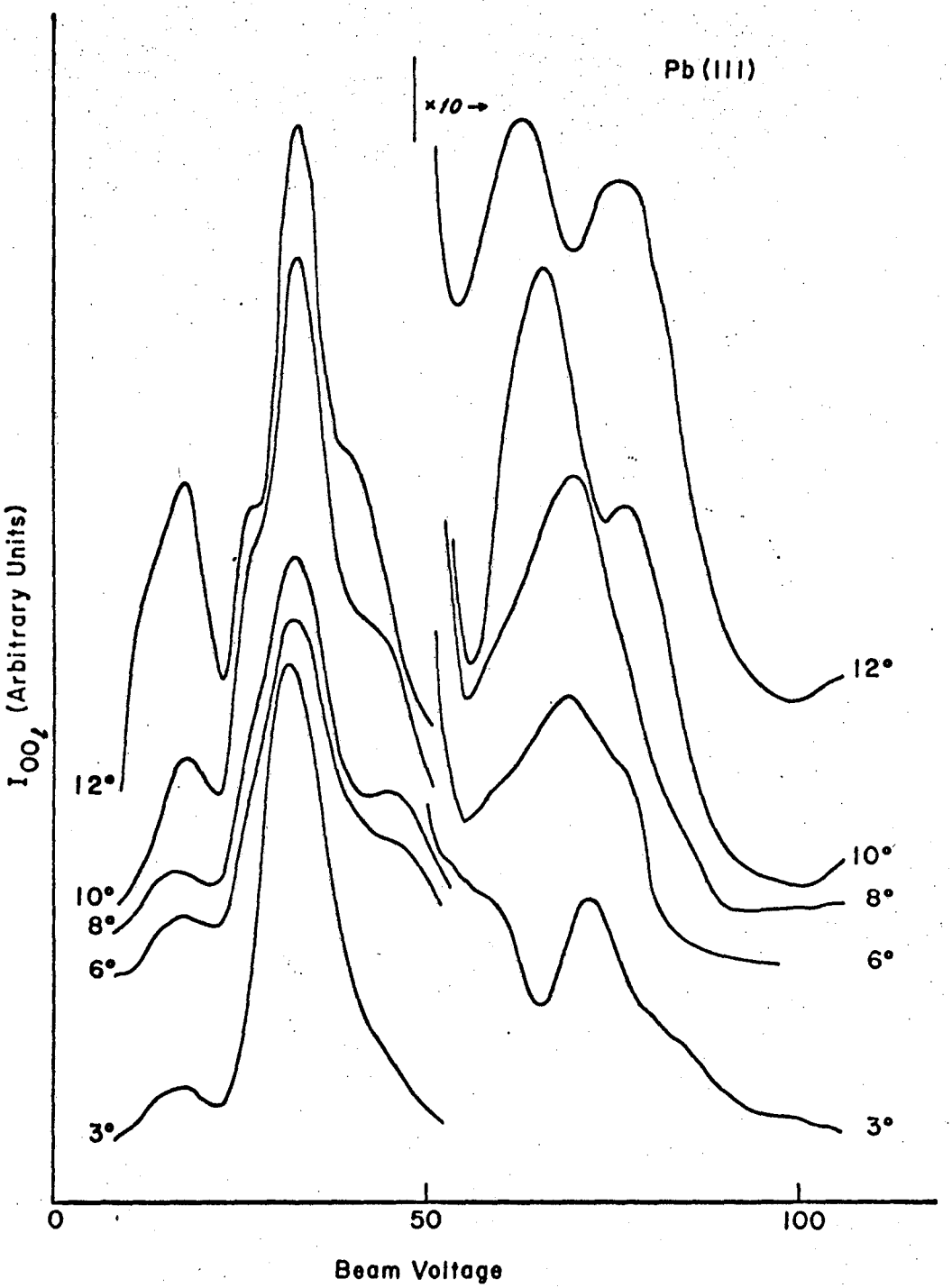

XBL 681-24

Fig. A-2 Specular intensity as a function of beam voltage for (111) face of lead at different angles of incidence.